

Analytical and Experimental Study of Condensation and Collapse of Steam Bubbles at High Jakob Number

S. Mambelli^{1*}; A. Ponomarev¹; Y. Sato¹; K. Mikityuk¹

¹Paul Scherrer Institute, Villigen PSI 5232, Switzerland
*Corresponding Author, E-mail: simone.mambelli@psi.ch

Abrupt collapse of vapour bubbles at high Jakob number is the leading physical phenomenon of the simulated chugging sodium boiling regime occurring during unprotected loss of flow (ULOF) accident in Sodium Fast Reactor (SFR) low-void core designs. The ESFR-SMART Horizon 2020 project aims at a better understanding and simulation of chugging conditions. Therefore, the small-scale two-phase flow facility “CHUG” for the mock-up of sodium boiling using water as sodium simulant has been designed at Paul Scherrer Institut (PSI) and built at the Laboratory of Reactor Systems behaviour at EPF Lausanne. CHUG consists of an acrylic glass test section filled with water at ambient temperature and atmospheric pressure, where high-temperature steam is injected from the bottom in order to study the interaction between vapour and liquid at high sub-cooling level. In this paper the experimental results obtained with CHUG facility are compared with the simulation of bubble collapse in sub-cooled liquid at high Jakob number performed with PSI’s in-house CFD tool PSI-BOIL. The three-dimensional bubble surface during formation and collapse at the orifice is obtained from high-speed imaging and compared to the results from PSI-BOIL simulation, where an interface tracking method based on third-order accurate CIP-CSL2 (Constrained Interpolation Profile – Conservative Semi-Lagrangian 2nd order) method is employed. The main features of inertia-driven bubble collapse are analysed and commented in both cases.

KEYWORDS: bubble dynamics, condensation, inertial collapse, two-phase flow

1. Introduction

The ESFR-SMART (European Sodium Fast Reactor Safety Measures Assessment and Research Tools) project aims at the further improvement of the safety of the commercial-size European Sodium Fast Reactor (ESFR) [1]. Among its main objectives, particular focus is set on the validation and calibration of the computational tools employed for the safety analyses. In order to support and validate these tools, several experimental campaigns are envisaged by the ESFR-SMART project.

In this framework the evaluation and simulation of such severe accident scenarios as the Unprotected Loss of Flow (ULOF) must be supported with new experimental data. Recent safety studies on the low-void SFR design have highlighted the potential occurrence of a stabilized chugging boiling regime during ULOF transient [2]. This regime may act as a level of defence preventing core melting. The driving physical phenomenon leading to the periodical expulsion and re-entering of liquid sodium in the fuel channels is the condensation of vapour at high Jakob number (Ja), which represents the ratio between the sensible heat and the latent heat both released by the bubble during the condensation process. Collapse of vapour bubbles at high Ja is called “inertial” because it is controlled by the inertia of the liquid mass accelerating in form of jets into the space left free by the condensing vapour [3].

In order to get new experimental data on the inertial collapse, a new experimental facility named CHUG was designed at Paul Scherrer Institut (PSI) and built at the Laboratory of Reactor Physics and Systems Behaviour of École Polytechnique Fédérale Lausanne (EPFL). CHUG consists of a vertical pipe made of acrylic glass filled with water at standard conditions (ambient temperature and atmospheric pressure). High-temperature steam is injected in the lower part of the test section in order to obtain fast bubble collapse recorded by the use of a high-speed camera. Pressure at the bottom of the section and the axial thermal stratification are recorded as well by dedicated sensors.

The experimental data obtained by CHUG will be compared with the results from PSI’s in-house CFD tool PSI-BOIL, in order to validate the code and obtain useful correlations related to the condensation process. The final aim will be the extrapolation of correlations from water to sodium with the purpose

of validating thermal-hydraulics codes employed for the safety analysis of the ULOF transient in ESRF.

2. CHUG: Experimental Setup

CHUG experimental setup is shown in Figure 1. The test section is a vertical pipe made of acrylic glass, with height of 2 meters and inner diameter of 54 mm, filled with water at ambient temperature and atmospheric pressure, where high-temperature steam is injected upwards at the bottom through a dedicated steam line. The steam line is also employed for the operations of refill and discharge of water in the test section. The steam is injected into the system through the use of a steam generator, able to turn service water into steam at a pressure of 6 bar. Acrylic glass was chosen in order to enable visualization of the bubble growth and collapse processes through the use of a high speed camera, while withstanding mildly harsh conditions (temperature up to 130°C and pressure up to 10 bar). The high speed camera (HSC) employed during the experimental test is the model HighSpeedStar 5.1 from LaVision, with a resolution of 1024x1024 pixels and a frame rate of 2 kHz, leading to a spatial resolution of 42 μm per pixel. The high speed camera is operated by the LaVision DaVis 8 software. A LED panel with a diffusive luminous flux of 4400 lm is placed behind the test section facing the high speed camera in order to enhance the image contrast.

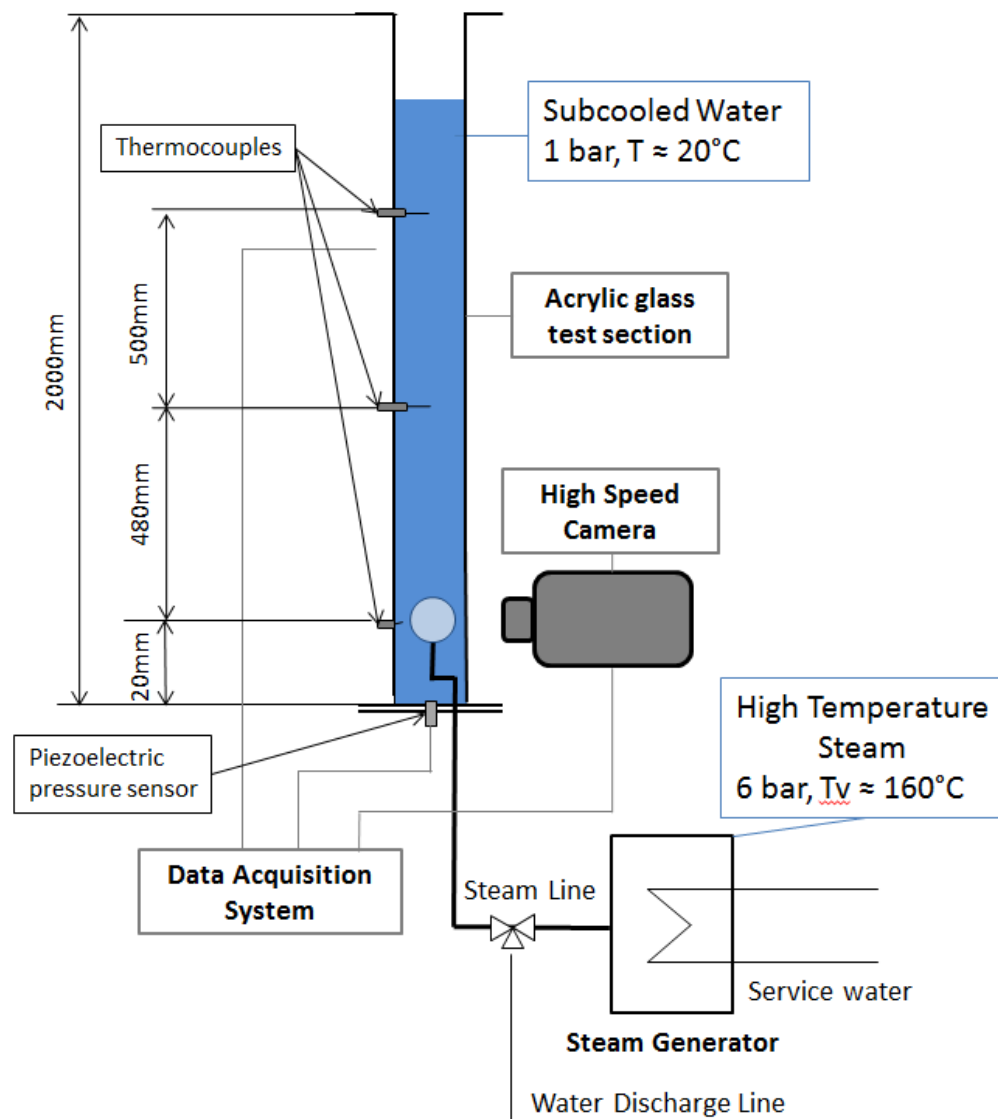


Figure 1: Scheme of the experimental setup of CHUG facility.

The measurement system is composed by a high-frequency piezoelectric pressure sensor fixed at the test section bottom and three thermocouples positioned on the test section wall at three different axial positions (height = 20 mm; 500 mm; 1000 mm). The pressure sensor allows the detection of pressure pulses released during the collapse of the bubble, while the thermocouples enable the tracking of the thermal stratification inside the test section during the experiment. In particular, the lowest thermocouple is placed at the injection level in order to measure the temperature of water near the bubble. Each of the sensors is connected to the data acquisition system, which is in turn connected to a dedicated computer controlling the data acquisition operations.

The experimental procedure is conducted as follows. The test section is refilled with distilled water until an axial set-point equal to a water level of 1.6 m. After turning on the steam generator, the temperature at the injection line inlet is measured via a portable thermocouple, while steam is damped outside the facility. Then, the injection line valve is opened for the start of the test. During the whole test, temperature and pressure are recorded and checked not to exceed the limits given by the optimal working conditions of the measurement equipment. At a selected instant, the high speed camera is triggered by a 5V square wave signal via a trigger generator sending signal at the same time to the data acquisition system and allowing the synchronization with the pressure data. When the test is over, the final water level is measured in order to estimate the average injection mass flow during the test. Finally, the test section is voided and cooled for the preparation of a new test.

3. Experimental Results

The aim of the experiment was the visual recording of steam bubble collapse at high Jakob number. The parameters of the experimental test at the beginning of the experiment are reported in Table 1. The HSC was triggered at $t = 45$ s after the start of the steam injection and it acquired frames for a period of 5 seconds. In Figures 2 and 3 the pressure and the temperature signals acquired by the previously described sensors are reported during the 5 seconds of image acquisition. It must be mentioned that only the dynamic pressure is detected and that the measurement has been corrected to take into account the temperature-induced drift on the sensor. More details on the correction of the temperature-induced drift can be found in the description of the previous CHUG experimental campaign in the main author's Master's Thesis [4].

As visible from Figure 2, high-frequency pressure oscillations with maximum at approximately 1 bar highlight the presence of the so-called regime of condensation oscillations [5]. The pressure positive and negative peaks correspond to the bubble collapse and growth, respectively. In particular, the highest pressure spikes occur when the steam re-enters downward the injection channel, causing the development of a strong pressure wave [6].

Experimental Test	
Parameter	Value
Steam Generator Pressure	6 ± 0.3 bar
Steam mass flow rate	1.5 ± 0.10 g/s
Steam Temperature at TS inlet	130 ± 2 °C
Pressure sampling frequency	26'800 Samples/s
Temperature sampling frequency	3 Samples/s
HSC sampling frequency	2'000 fps

Table 1 : List of experimental parameters employed during the test in CHUG facility.

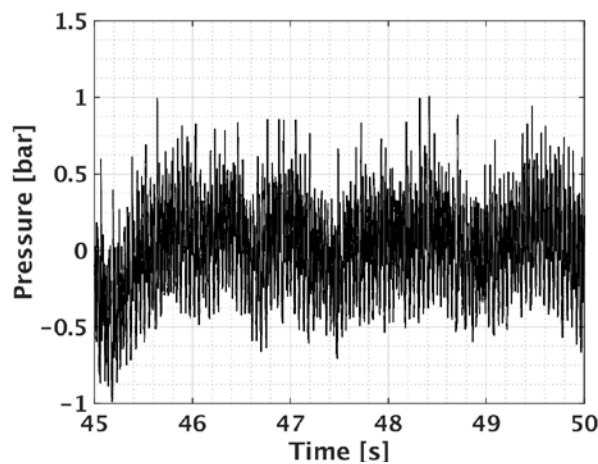


Figure 2: Dynamic measurement of pressure oscillations acquired during HSC frame acquisition: the temperature drift has been corrected.

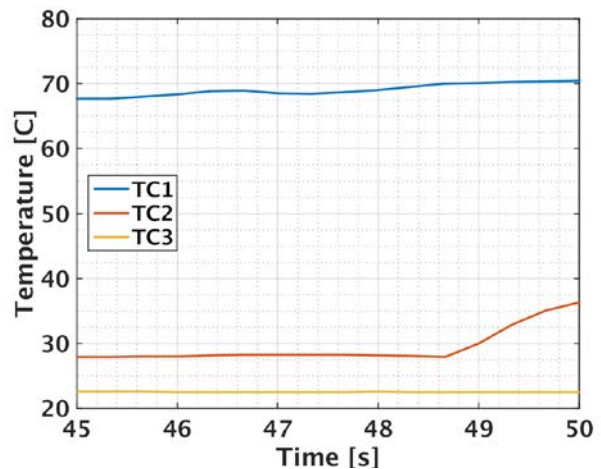


Figure 3: Temperature measurement acquired during HSC frame acquisition at three different axial positions.

In Figure 3 the temperature recorded during HSC frame acquisition at three different axial locations is displayed. It is visible how in a short window of time the temperature can be considered constant. Only the temperature at the injection level slowly increases constantly over time, while the temperature at the intermediate position starts increasing only from approximately $t = 49$ seconds on. This highlights the presence of a sizeable thermal stratification developing during the test. This may play an important role for the validation of thermal hydraulics codes, where thermal stratification is usually hard to achieve due to the smearing of the colour function [4, 7]. The temperature at the injection level is approximately equal to 70°C , leading to an actual Jakob number at the moment of image recording equal to about 110. This is higher than the threshold of $Ja = 100$, which separates the thermally-driven collapse and the inertial one [8].

The collapse of bubbles at high sub-cooling is indeed characterized by negligible heat transfer effects and predominance of liquid inertia effects. The theoretical behaviour of inertial collapse was described firstly by Lord Rayleigh, who provided a mathematical solution for spherical bubble collapse [9]. However, due to the profoundly instable behaviour of the bubble surface during the collapse, the bubble tends to break up into several small bubbles. This may be due the development of harmonic disturbances on the bubble surface, like in case of Microbubble Emission Boiling (MEB) [10], or due to the formation of an upward jet caused by an asymmetry such as the presence of the hydrostatic gradient [11].

In Figure 4 the evolution of the inertial collapse of a steam bubble, as recorded by the HSC, is displayed. First of all it must be noticed that the test section contains a sizeable quantity of air bubbles. Air entrance inside the facility disturbs the visualization of steam bubbles while damping the magnitude of the pressure waves propagating from the collapse. However, their presence does not play a significant role in the behaviour of the bubble surface; therefore they do not invalidate the study. In the future a deaerator is planned to be included in the experimental setup.

The bubble completely develops and collapse in approximately 10 ms. Its form is not spherical but rather flattened along the vertical direction, assuming a pseudo-ellipsoidal which tends to encapsulate the injection pipe. Throughout its life, the bubble shows very fine disturbances on its surface, causing the interface to be highly unstable. If compared to the experimental bubble in [10], the disturbances are considerably finer and spread across the entire surface of the bubble, not only on the top. However, it is interesting to notice how the final break-up of the bubble leads to the formation of a large number of microbubbles, as predicted by MEB and visible from $t^* + 9.0$ ms on.

On the other hand, it is possible to notice how the final break-up of the bubble occurs at the moment of the detachment from the injection nozzle. While the bubble is attached to the orifice, an inferior inward recess is formed on both sides of the bubble, due to the strong condensation effects given by the high Jakob number. As soon as the bubble detaches from the orifice, the hydrostatic pressure gradient

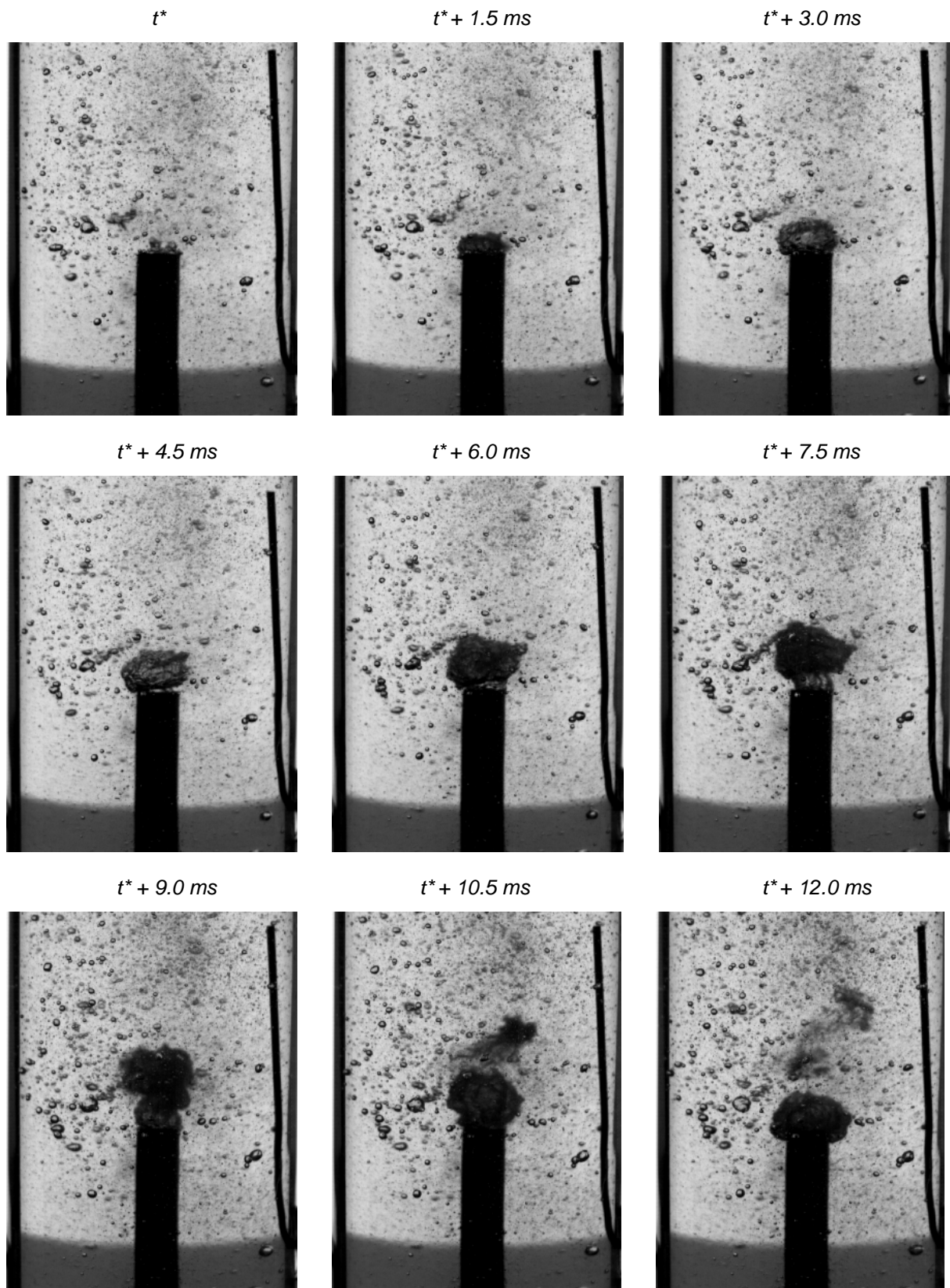


Figure 4: Example of the evolution of the growth and collapse of steam bubbles during CHUG experimental test, as recorded by the high speed camera. t^* is an arbitrary time instant when the steam-water is still contained inside the injection nozzle.

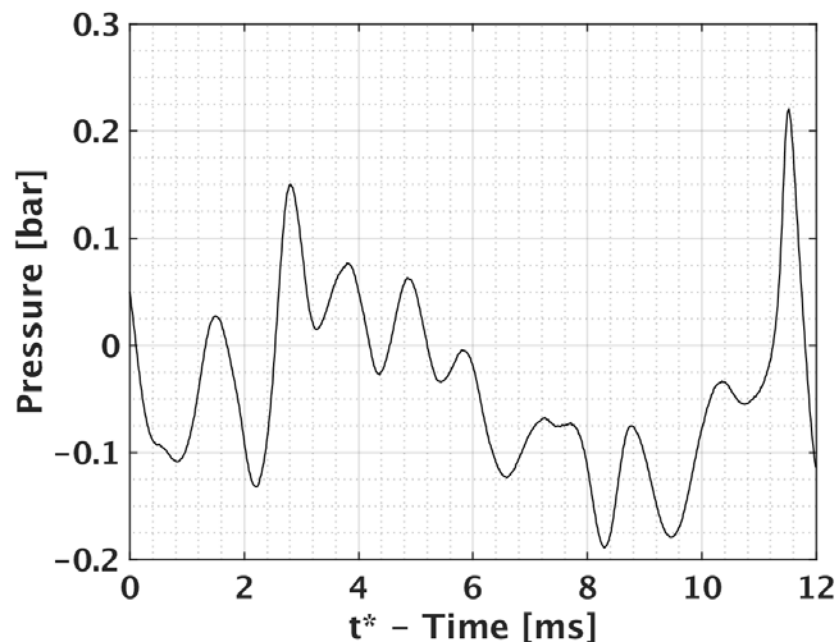


Figure 5: Dynamic measurement of pressure oscillations corresponding to the time interval of the frames of Figure 4: the temperature drift has been corrected. t^* corresponds to the same time instant of Figure 4.

gives an upward impulse to the top part of the interface, while at the bottom the liquid is accelerated toward the voided space left by the condensed steam. This results in an upward liquid micro-jet which is barely visible from Figure 5 but which is the cause for the final break-up into hundreds of micro-bubbles.

Finally, it must be noticed that right after the collapse of the first shown bubble, a second bubble rapidly develops and breaks up as well into micro-bubbles (between $t^* + 10.5$ ms and $t^* + 12$ ms). The high-frequency development of bubbles in series is one of the main characteristics of condensation oscillations and is caused by two main factors: the high steam injection mass flow rate; the acceleration due to the presence of the wake of the previous collapsed bubble. Figure 5 shows the pressure measurement during the bubble evolution depicted in Figure 4. It is visible how oscillations with frequency of the order of 1 kHz develop throughout the bubble growth and collapse, due to the movement of the interface. It must be noticed that during the strong condensation process causing the development of the inward recess at the bottom of the bubble (from $t^* + 6.0$ ms on) a depression is formed. On the other hand, the collapse of bubbles generates pressure spikes, as noticeable from $t^* + 9.0$ ms on. In particular, the pressure spike caused by the fast collapse of the second bubble, which is accelerated in the wake of the first bubble, is significantly stronger. This behaviour is one of the main reasons leading to the high-frequency pressure oscillations shown in Figure 2.

4. PSI-BOIL simulation of condensing bubble collapse under CHUG conditions

PSI-BOIL (Parallel Simulator of BOILING phenomena) is a three-dimensional, numerical CFD solver for multiphase flows in presence of heat transfer and phase change [12]. Second order accurate Finite Volume (FV) method on staggered orthogonal grids is employed for space discretization while time discretization is based on the fractional step method [13] (also called projection method). The interface tracking is performed through the CIP-CSL2 method (Constrained Interpolated Profile method: Conservative Semi-Lagrangian 2nd order scheme) [14].

As already mentioned above, the final aim of the CHUG project will be the extrapolation of useful correlations regarding condensation during inertial collapse for sodium, using water as a simulant. In previous studies the use of water as a sodium simulant has already been justified [15, 16]. However, before implementing sodium properties in PSI-BOIL and simulating inertial collapse in sodium, it is fundamental to verify if all the features of bubble collapse at high Jakob number are reproduced by the

Property	Water	Steam
Pressure	1 bar	5 bar
Temperature	20°C	151.8° C
Viscosity	0.001 Pa·s	1.396×10^{-5} Pa·s
Density	$1000 \frac{kg}{m^3}$	$2.668 \frac{kg}{m^3}$
Specific Heat Capacity (C_p)	$4184 \frac{J}{kg \cdot K}$	$2410 \frac{J}{kg \cdot K}$
Thermal Conductivity	$0.600 \frac{W}{m \cdot K}$	$0.03025 \frac{W}{m \cdot K}$
Saturation Temperature		100°C
Surface Tension		$0.059 \frac{N}{m}$
Latent Heat		$2.258 \times 10^6 \frac{J}{kg}$

Table 2: Input parameters for the simulation of condensing bubble performed by PSI-BOIL [4].

code. That is why the experimental results shown in the previous section are compared to the set of PSI-BOIL simulations performed in frame of the Master's Thesis project of the main author [4].

The input parameters of the simulation of condensing bubble collapse taken under consideration in this analysis are shown in Table 2 [4]. Steam (151.8°C, corresponding to the saturation temperature at 5 bar) is injected upwards with a velocity equal to 1 m/s into a column of water at standard conditions (20°C, 1 bar) through a squared orifice placed at the bottom. This situation corresponds to a Jakob number equal to 148. The computational domain consists of a parallelepiped of dimensions 2 cm×2 cm×8 cm, distributed among 64×64×256 cells, with the squared aperture at the bottom of the water column scaling to 3.75 mm×3.75 mm (12×12 cells).

It must be pointed out that the conditions of the simulation do not coincide with the actual experimental conditions presented in the previous section, but are considered because they emphasize all the features of the inertial collapse. This comparison serves only to highlight the possible prediction of the collapse characteristics compared to what is observed experimentally. A best estimate analysis with PSI-BOIL is foreseen in the future in the framework of the CHUG project.

Prior to the presentation of the simulation results, it is necessary to point out the actual capabilities of PSI-BOIL in the reproduction of bubble collapse. First of all, it must be highlighted that at the moment PSI-BOIL is able to treat only incompressible fluids. This means that all the phenomena involving compressibility and propagation of pressure waves are not simulated. For instance the Rayleigh solution [9] for the inertial collapse of spherical bubbles cannot be entirely reproduced, since it involves a stage where compressibility plays a fundamental role. However, thanks to the highly efficient interface and phase change models introduced in the code, the bubble surface disturbances and the effects of liquid inertia on the bubble break-up can be reproduced by PSI-BOIL. Unfortunately, the coarse grid domain chosen for this simulation does not allow the detailed solving of the thermal boundary layer and the reproduction of the very fine disturbances developing on the bubble surface before the break-up into micro-bubbles. A fine grid calculation is envisaged as future step of the CHUG project.

Figure 6 shows the evolution of the bubble over time as calculated by PSI-BOIL. As it was just explained, the coarse grid representation does not enable the reproduction of the fine disturbances on the bubble surface as in experimental conditions. However, while the bubble growth is considerably slower, it is noticeable how the break-up of the steam bubble occurs in the same time scale as in the experimental test, although both the Jakob number and the injection mass flow are significantly different. This highlights how the inertial collapse is not driven by the temperature difference nor by the steam inlet velocity, but rather by the impulses on the bubble interface given by the surface tension and the hydrostatic pressure gradient. Coarse disturbances are anyway created during the process of bubble detachment, due to the upward impulse given by the hydrostatic pressure gradient and by the formation of the inferior inward recess due to the strong condensation.

At the end of the bubble life, a liquid micro-jet forms upwards from below the surface, causing the bubble to break-up in several small ones. Obviously the presence of the final micro-bubbles viewed during the experimental test cannot be reproduced due to the coarse grid arrangement, but the overall collapse features are accurately reproduced.

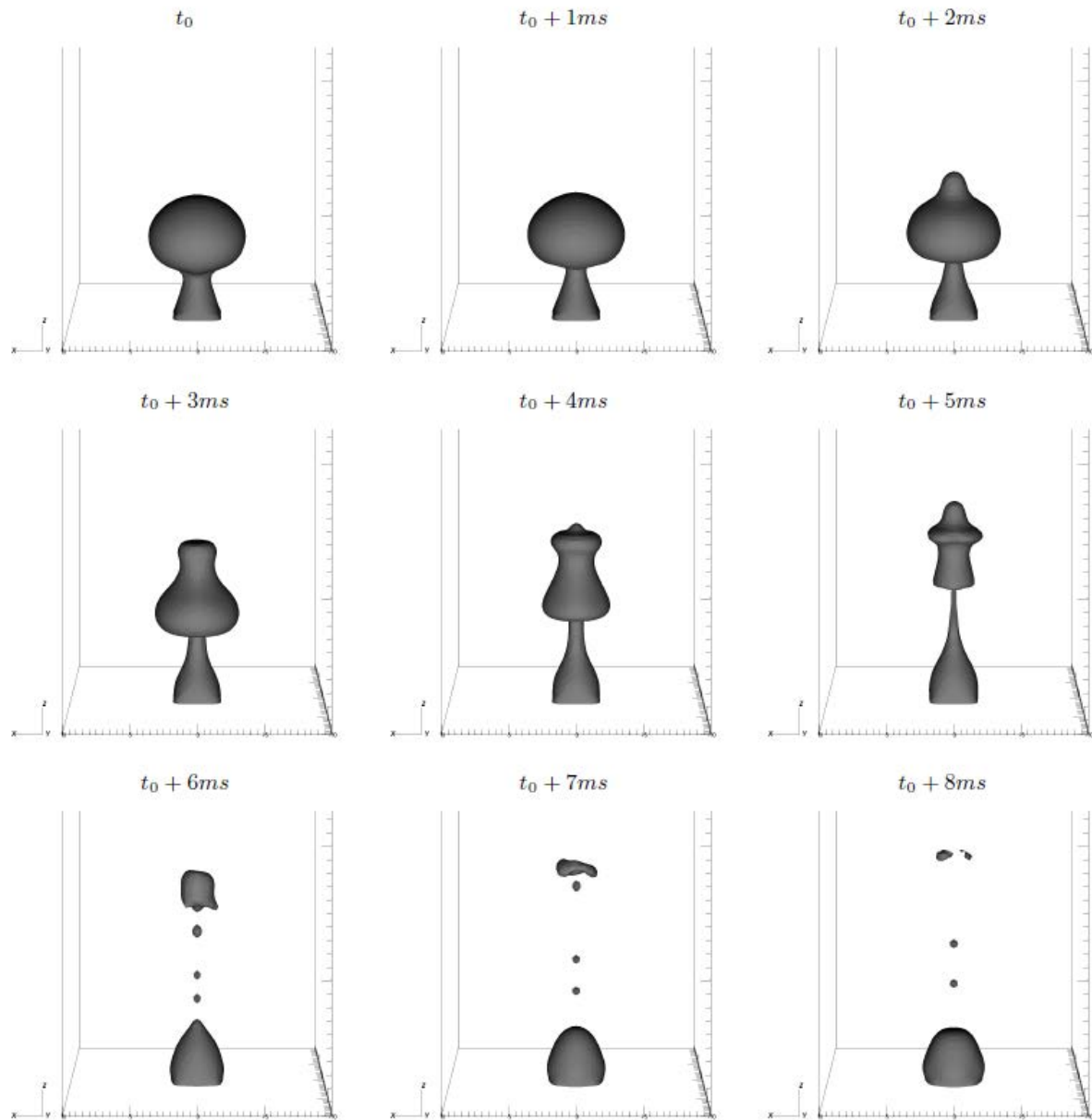


Figure 6: Example of the evolution of the growth and inertial collapse of a steam bubble, as simulated by PSI-BOIL [4]. t_0 is an arbitrary time instant when the bubble has reached its maximum volume.

5. Conclusion

The main objective of the analysis presented in this paper was to highlight the possibility to obtain a good reproduction of the main features of the inertia-driven bubble collapse, previously recorded via the employment of a high speed camera on CHUG experimental facility, with PSI's in-house CFD code PSI-BOIL.

First of all, CHUG facility is able to reproduce and therefore to gather new experimental data on the characteristics of inertial bubble collapse, which is the main condensation mechanism occurring during sodium boiling in ULOF transient. The employment of the acrylic glass test section and the high speed camera gives a number of directions along which the study of bubble collapse can be improved. For instance, through the employment of a system of mirrors it is possible to get multiple views that would enable the employment of an orthogonal imaging algorithm. This would give the opportunity to extract fundamental data from the behaviour of the bubbles, such as the evolution of their volume over time.

On the other hand, PSI-BOIL has demonstrated to be a powerful tool in the simulation of the bubble surface behaviour. The inertia-driven collapse time scale has been perfectly reproduced as well as the break-up of the main bubble due to the formation of an upward liquid micro-jet. This means that the code can be employed for future best estimate analyses by matching the experimental conditions and employing a finer grid. The final step in this direction will be the implementation of sodium properties into the code for the sake of simulating condensation events occurring in liquid metal. This would give very useful information about sodium boiling behaviour and can be turned into useful correlations to be applied to thermal-hydraulics codes.

Acknowledgment

The work has been prepared within EU Project ESFR-SMART which has received funding from the EURATOM Research and Training Programme 2014-2018 under the Grant Agreement No. 754501.

We especially thank Dr. Pavel Frajtag and Daniel Godat from École Polytechnique Fédérale Lausanne (EPFL) for the assistance with the setup of CHUG experimental facility.

We would also like to show our gratitude to Petros Papadopoulos, Doctorand at Eidgenössische Technische Hochschule Zürich, for the introduction and the advices on the use of the high speed camera used for the experimental test.

References

- [1] K. Mikityuk, E. Girardi, J. Krepel, E. Bubelis, E. Fridman, A. Rineiski, N. Girault, F. Payot, L. Buligins, G. Gerbeth, N. Chauvin, C. Latge and J.-C. Garnier, "ESFR-SMART: new Horizon-2020 project on SFR safety," in *International Conference on Fast Reactors and Related Fuel Cycles: Next Generation Nuclear Systems for Sustainable Development (FR17)*, Yekaterinburg, Russia, 26-29 June 2017.
- [2] N. Alpy, P. Marsault, M. Anderhuber, A. Gerschenfeld, P. Sciora, D. Kadri, J. Perez and R. Lavastre, "Phenomenological investigation of sodium boiling in a SFR core during a postulated ULOF transient with CATHARE 2 system code: a stabilized boiling case," *Journal of Nuclear Science and Technology*, vol. 53:5, pp. 692-697, 2015.
- [3] F. Mayinger and Y. Chen, "Heat transfer at the phase-interface of condensing bubbles," in *Proceedings Eight International Heat Transfer Conference*, San Francisco, California, 1992.
- [4] S. Mambelli, "Analytical and Experimental study of chugging boiling instability: the CHUG project," Master's Thesis - Eidgenössische Technische Hochschule Zürich, <https://doi.org/10.5281/zenodo.1311464>, 2018.
- [5] I. Aya and H. Nariai, "Boundaries between Regimes of Pressure Oscillation induced by Steam," *Nuclear Engineering and Design*, vol. 99, pp. 31-40, 1987.
- [6] C. E. Brennen, *Fundamentals of Multiphase Flows*, Pasadena, California: California Institute of Technology: Cambridge University Press ed., 2008.
- [7] T. Norman, H. Park, S. Revankar, M. Ishii and J. Kelly, "Thermal stratification and mixing in an open water pool by submerged mixtures of steam and air," in *Proceedings of the ASME International Mechanical Engineering Congress and Exposition (IMECE 06)*, 2006.
- [8] F. Mayinger and Y. Chen, "Heat transfer at the phase-interface of condensing bubbles," in *Proceedings Eighth International Heat Transfer Conference*, San Francisco, California, 1986.
- [9] L. Rayleigh, "Pressure Developed in a Liquid During the Collapse of a Spherical Cavity," *Philosophical Magazine*, vol. 34, pp. 94-98, 1917.
- [10] I. Ueno, Y. Hattori and R. Hosoya, "Condensation and Collapse of Vapor Bubbles Injected in Subcooled Pool," *Microgravity Science Technology*, vol. 23, pp. 73-77, 2011.
- [11] T. Benjamin and A. Ellis, "The Collapse of Cavitation Bubbles and the Pressures thereby produced against Solid Boundaries," *Philosophical Transactions Royal Society*, Vols. A-260, pp. 221-240, 1966.
- [12] Y. Sato and B. Niceno, "A sharp-interface phase change model for a mass-conservative interface tracking method," *Journal of Computational Physics*, vol. 249, pp. 127-161, 2013.
- [13] A. Chorin, "Numerical solution of the Navier-Stokes equations," *Mathematics of Computation*, vol. 22, pp. 745-762, 1968.

- [14] T. Nakamura, B. Tanaka, T. Yabe and K. Tazikawa, “Exactly conservative semi-lagrangian scheme for multi-dimensional hyperbolic equations with directional splitting technique,” *Journal of Computational Physics*, vol. 174, pp. 171-207, 2001.
- [15] T. S. Playle, “Simulation of sodium boiling using a water model: voiding and re-entry processes,” *Chemical Engineering Science*, vol. 28, pp. 1199-1211, 1973.
- [16] S. J. Board and R. B. Duffey, “Spherical bubble growth in superheated liquids,” *Chemical Engineering Science*, vol. 26, pp. 263-274, 1971.